Important role of the Beckmann rearrangement in the gas phase chemistry of protonated formaldehyde oximes and their $[CH_4NO]^+$ isomers

Minh Tho Nguyen, Greet Raspoet and Luc G. Vanquickenborne
Department of Chemistry, University of Leuven, Celestijnenlaan 200F, B-3001 Leuven, Belgium

The $[CH_4NO]^+$ potential energy surface has been (re)examined in detail using *ab initio* molecular orbital calculations. Geometries of the stationary points were optimized at the MP2/6-31G(d,p) level. On the basis of MP4SDTQ/6-311++G(2d,2p) electronic energies with zero-point corrections, the following heats of formation at 0 K could be proposed: $\Delta_f H^\circ_0$ in kJ mol^{-1}: $H_2C{=}NOH$: 31 ± 12; $H_3C{-}N{=}OH^+$: 903 ± 12; $H_2C{=}NH{-}OH^+$: 759 ± 12; $H_2C{=}N{-}OH_2^+$: 838 ± 12; $H_3C{-}NH{=}O^+$: 840 ± 12 and cyclic $H_2C{-}NH{-}OH^+$: 918 ± 12. The proton affinities could also be evaluated: $E_{PA}(H_2C{=}NOH) = 799 \pm 12$ kJ mol^{-1} and $E_{PA}(CH_3{-}N{=}O) = 763 \pm 12$ kJ mol^{-1}. Energies of the transition structures of several unimolecular rearrangements and fragmentations obtained using MP4SDTQ/6-311++G(d,p) + ZPE calculations suggest that the following sequence of transformations is the most energetically favoured route: protonation of formaldehyde oxime ⟶ *N*-protonated oxime ⟶ *O*-protonated oxime ⟶ fragmentation products ($HCN + H_3O^+$). The 1,2-H-shift connecting both protonated forms constitutes the rate-controlling step. The classical Beckmann rearrangement of the *O*-protonated formaldehyde oxime is the most facile reaction of all the paths considered and should thus play an important role in the gas phase unimolecular chemistry of the $[CH_4NO]^+$ ion isomers. The $CH_4 + NO^+$ reaction has also been examined as a simple model for the electrophilic substitution of aliphatic hydrocarbons. While the insertion of NO^+ into a C–H bond can be established, the evidence recently reported for preferential attack of NO^+ on the carbon atom could not be confirmed.

In spite of the large amount of results that have been reported during the past century on the synthetic and industrial applications of the Beckmann rearrangement[1,2] of oximes, the mechanistic aspects of this reaction remain poorly understood. Although the rate constants and the associated activation energies could be measured in many cases,[3] the nature of the rate-determining step of the Beckmann rearrangement (BR) has not been identified yet. It has commonly been assumed that the process begins with a protonation at the oxygen centre of an oxime followed by a migration from carbon to nitrogen of a group *anti* to the hydroxy group [reaction (1)].

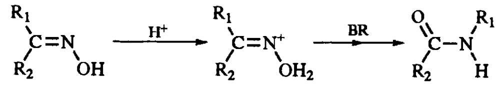

$$\mathrm{R_1R_2C{=}N{-}OH \xrightarrow{H^+} R_1R_2C{=}N^+{-}OH_2 \xrightarrow{BR} O{=}C(R_2){-}N(R_1)H} \quad (1)$$

In a recent preliminary theoretical study,[4] we have shown that *N*-protonation of formaldehyde oxime should be largely preferred over the *O*-protonation. In its simplest model case, the energy difference between both *N*- and *O*-protonated forms amounts to *ca.* 77 kJ mol^{-1} in favour of the *N*-protonated form. On the other hand, the energy barrier for the BR [reaction (2)]

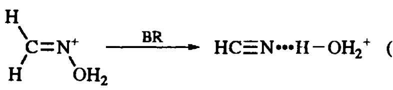

$$\mathrm{H_2C{=}N^+{-}OH_2 \xrightarrow{BR} HC{\equiv}N\cdots H{-}OH_2^+} \quad (2)$$

of the *O*-protonated form has been calculated to be only 44 kJ mol^{-1} at the MP4/6-311++G(d,p) + ZPE level of molecular orbital theory. The latter is thus smaller than the experimental activation energies of *ca.* 100 kJ mol^{-1} measured for several oximes in different solvents.[3]

These differences raise a number of fundamental questions about the BR mechanism, namely, (*i*) the identity of the rate-determining step; (*ii*) the influence of the substituents at both N and C centres; and (*iii*) the effect of the solvent used.

The purpose of the present work is an attempt to tackle the first question in establishing the eventual interconnections between the BR and other transformations involving protonated oximes. The results obtained for formaldehyde oxime will serve as a reference for future study on the second and third question. In the meantime the present study also emphasizes an important role played by the BR in the gas phase reactivity of the $[CH_4NO]^+$ ion isomers. In fact, a recent study[5] showed that the gas phase BR offers a better rationalization for the loss of HCN from metastable hydrazonium cation analogues ($CH_2{=}N{-}NH_3^+$) than the 1,2-*cis* elimination. On the other hand, the $CH_4 + NO^+$ reaction is also of interest with regard to the electrophilic nitrosation of hydrocarbons.[6]

Calculations

Ab initio molecular orbital (MO) calculations were performed with the aid of a local version of the GAUSSIAN 90 set of programs.[7] The stationary points on the $[CH_4NO]^+$ potential energy surface were initially located and characterized by harmonic vibrational analysis at the Hartree–Fock (HF) level with the split-valence plus dp-polarization 6-31G(d,p) basis set. Geometries of the relevant equilibrium and transition structures were then reoptimized at the second-order Møller–Plesset perturbation theory (MP2) level with the same atomic functions. Improved relative energies between the stationary points were subsequently estimated using full fourth-order perturbation calculations (MP4SDTQ) in conjunction with the larger 6-311++G(d,p) basis set (++ indicates a set of sp-diffuse functions on C and N and s-diffuse functions on H) at MP2/6-31G(d,p)-geometries and corrected for zero-point

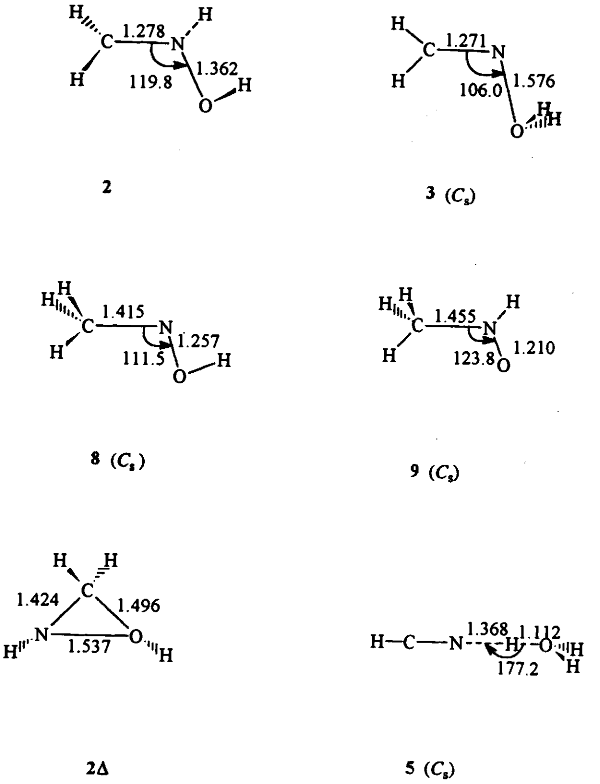

Fig. 1 Selected MP2/6-31G(d,p)-geometries of the $[CH_4NO]^+$ equilibrium structures

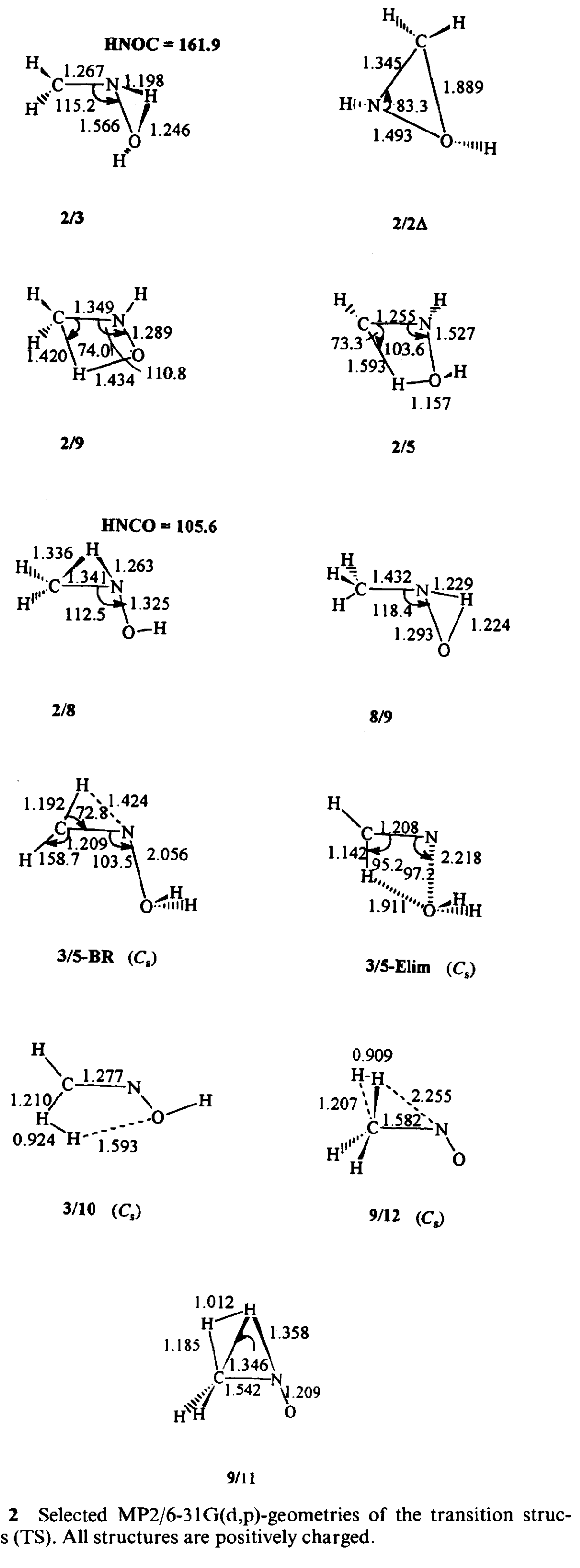

Fig. 2 Selected MP2/6-31G(d,p)-geometries of the transition structures (TS). All structures are positively charged.

vibrational energies (ZPE). In order to estimate the heats of formation of the equilibrium structures and the proton affinities, calculations using a larger basis set, 6-311++G(2d,2p), were also carried out. Throughout this paper, total energies are given in hartrees, relative and zero-point energies in kJ mol^{-1}, bond lengths in Å and bond angles in degrees.

Results and discussion

To faciliate comparison with results reported in our previous paper,[4] we have adopted a similar numbering for the structures displayed in Scheme 1. Formaldehyde oxime **1** contains in principle three distinct sites of protonation: the *N*-, *O*- and *C*-protonations could thus lead to the formation of the methyleniminium **2**, hydroxonium **3** and nitrosonium **8** cations, respectively. The ion **8** is also the *O*-protonated form of nitrosomethane (CH_3–N=O) whose corresponding *N*-protonation could also generate **9**. The three-membered cycle **2Δ** (Δ stands for a ring) is related to **2** through a simple ring-closure. The four isomers **2**, **3**, **8** and **9** are linked to each other by direct or successive 1,2- or 1,3-shifts of the hydrogen. As shown in ref. 4, the ion-molecule complex **5** between the fragments **6** ($HCNH^+ + H_2O$) is not only the primary product of the BR of the *O*-protonated **3** but also the common complex resulting

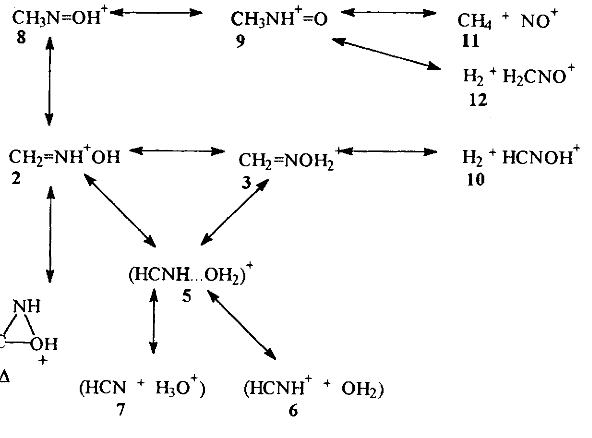

Scheme 1

Table 1 Total, zero-point vibrational and relative energies of the $[CH_4NO]^+$ ion structures

Structure[a]	[MP4SDTQ/ 6-311++G(d,p)]/ hartree[b]	ZPE/ kJ mol^{-1}[c]	Relative energy/kJ mol^{-1}	
			MP4	MP4 + ZPE[d]
$H_2C{=}N{-}OH_2^+$ **3**	−169.748 13	143	0	0(0)
$H_2C{=}NH{-}OH^+$ **2**	−169.779 75	149	−83	−77 (−79)
$H_2\underbrace{C{-}NH{-}O}H^+$ **2Δ**	−169.720 49	150	73	80 (80)
$(HCNH^+\cdots OH_2)$ **5**	−169.844 86	133	−254	−264
$HCNH^+ + H_2O$ **6**	−169.794 49	127	−122	−138
$HCN + H_3O^+$ **7**	−169.790 86	130	−112	−125
$H_3C{-}N{=}OH^+$ **8**	−169.725 40	143	60	60 (65)
$H_3C{-}NH{=}O^+$ **9**	−169.750 21	145	−6	−3 (2)
$H_2 + HCNOH^+$ **10**	−169.686 97	108	161	126 (125)
$CH_4 + NO^+$ **11**	−169.734 76	127	35	19 (29)
$H_2 + H_2CNO^+$ **12**	−169.675 07	107	192	156 (184)
$CH_3^+ + NH{=}O$ **13**	−169.607 22	117	370	344 (349)
1,2-H TS **2/3**	−169.686 95	130	161	148
Ring-opening TS **2/2Δ**	−169.683 98	143	168	168
1,2-H TS **2/8**	−169.694 22	135	142	134
1,3-H TS **2/9**	−169.643 73	130	274	261
1,2-Elim TS **2/5**	−169.663 84	133	221	211
BR TS **3/5**-BR	−169.723 17	121	66	44
1,2-Elim TS **3/5**-Elim	−169.710 33	122	99	78
1,2-H TS **8/9**	−169.652 91	126	250	233
H_2-Elim TS **3/10**	−169.644 25	121	273	251
H_2-Elim TS **9/12**	−169.631 39	122	306	285
CH_4-Elim TS **9/11**	−169.607 80	122	368	347

[a] Based on MP2/6-31G(d,p)-geometries given in Figs. 1 and 2. [b] Core orbitals are frozen. [c] From HF-6-31G(d,p) calculations and scaled by 0.9. [d] Including MP4 relative energies and ZPE corrections. The values obtained from MP4SDTQ/6-311++G(2d,2p) + ZPE calculations are in parentheses.

from the fragments **7** ($HCN + H_3O^+$). On the other hand, **5** could also be obtained from either **2** or **3** by a 1,2-*cis*-elimination. The overall connections between $[CH_4NO]^+$ ion isomers considered in this work are shown in Scheme 1. In addition, a number of simple fragmentations of the isomers have also been examined. Fig. 1 displays the selected MP2/6-31G(d,p)-optimized parameters of the equilibrium structures whereas Fig. 2 records those of the transition structures (TS). In general, **X**/**Y** stands for a TS connecting both equilibrium structures **X** and **Y**. Parameters of the fragments are not included in Fig. 2. Corresponding total, zero-point vibrational and relative energies are summarized in Table 1. Schematic potential energy curves illustrating the unimolecular rearrangements are shown in Figs. 3, 4 and 5.

Stable $[CH_4NO]^+$ ion isomers

The structures **2**, **2Δ**, **3**, **5**, **8** and **9** represent local minima on the $[CH_4NO]^+$ potential energy surface. Let us first compare the calculated energies of some product fragments **6**, **7** and **10** for which experimental data are available. Owing to the fact that the proton affinity of HCN is somewhat larger than that of H_2O, the fragments **6** ($HCNH^+ + H_2O$) is lower in energy than **7** ($HCN + H_3O^+$). The following proton affinities are obtained using MP4/6-311++G(d,p) + ZPE calculations: E_{PA} (HCN) = 707 kJ mol^{-1} and E_{PA} (H_2O) = 694 kJ mol^{-1}; the corresponding experimental values are 712 and 692 kJ mol^{-1}, respectively.[8] However, the errors incurred by calculations are not systematic, the former being underestimated while the latter are overestimated. A cumulative effect thus gives a larger underestimation when comparing **6** and **7**. In fact, our estimation places **7** above **6** by 13 kJ mol^{-1}, whereas the experimental difference amounts to 20 kJ mol^{-1}. Concerning the NO^+ ion, it is established that the MP perturbation expansion is not well converged for this species. In any case, we could expect an average error of *ca.* ± 12 kJ mol^{-1} for heats of formation by calculations at the level of theory employed here.

There have been some previous MO calculations on the $[CH_4NO^+]$ species.[4,6,9] The complex **5** is by far the lowest energy minimum among the structures considered, lying 264 kJ mol^{-1} below the *O*-protonated form **3**. Of the three protonated forms **2**, **3** and **8** of formaldehyde oxime, the *N*-protonated **2** is as shown in ref. 4 largely favoured and followed by the *O*-form **3**. The *C*-protonated form **8** is rather a high-energy species. Relative to **3**, **2** lies 77 kJ mol^{-1} lower in energy, while **8** lies 60 kJ mol^{-1} higher. Only the *E*-conformation **8** is shown in Fig. 1; the corresponding *Z*-conformer also exists as a local minimum, but it is 32 kJ mol^{-1} less stable than **8**. As the *O*-protonated form of nitrosomethane, **8** also has a lower stability than the related *N*-protonated nitrosomethane **9** by 63 kJ mol^{-1}. The latter turns out to have an energy similar to **3**. The three-membered ring **2Δ** is a high-energy isomer lying 157 kJ mol^{-1} above **2**. It appears useful to estimate the heats of formation of the ion isomers. For this purpose, we have considered the following group exchange reactions and calculated their heats of reaction at 0 K using the electronic energies computed with a larger basis set, namely at the MP4SDTQ/6-311++G(2d,2p)//MP2/6-31G(d,p) + ZPE level. We thus obtain

$$H_2C{=}N{-}OH\ \mathbf{1} + H_2 \longrightarrow H_2C{=}NH + H_2O \quad (\Delta_rH = -174\ \mathrm{kJ\ mol^{-1}}) \tag{3}$$

$$H_2C{=}N{-}OH^+\ \mathbf{2} + H_2 \longrightarrow H_2C{=}NH_2^+ + H_2O \quad (\Delta_rH = -238\ \mathrm{kJ\ mol^{-1}}) \tag{4}$$

Together with the known experimental data $\Delta_fH^\circ_0$ at 0 K of H_2O, $H_2C{=}NH$ and $H_2C{=}NH_2^+$ being −239, 96 and 760 kJ mol^{-1}, respectively,[8,10] the above heats of reaction allow the heats of formation at 0 K of **1** and **2** to be evaluated: $\Delta_fH^\circ_0(H_2C{=}N{-}OH\ \mathbf{1}) = 31 \pm 12$ kJ mol^{-1}, $\Delta_fH^\circ_0(H_2C{=}NH{-}OH^+\ \mathbf{2}) = 759 \pm 12$ kJ mol^{-1}.

We note that an estimate of 29 kJ mol^{-1} for **1** has been

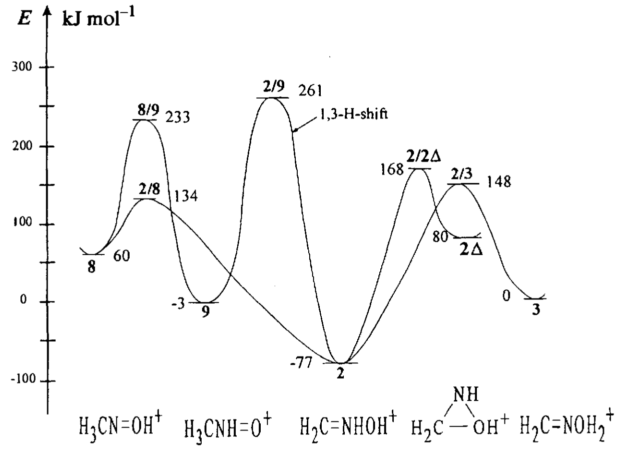

Fig. 3 Schematic potential energy profiles for interconversions between $[CH_4NO]^+$ ion isomers. Relative energies obtained from MP4/6-311++G(d,p) + ZPE calculations.

tentatively listed in the compilation by Lias *et al.*[8] Use of the relative energies at the MP4/6-311++G(2d,2p) + ZPE level listed in Table 1 leads to the heats of formation of other cationic isomers: $\Delta_f H^\circ_0(H_2C{=}N{-}OH_2^+\ \mathbf{3}) = 838 \pm 12$ kJ mol^{-1}, $\Delta_f H^\circ_0(H_3C{-}NH{=}O^+\ \mathbf{9}) = 840 \pm 12$ kJ mol^{-1}, $\Delta_f H^\circ_0(H_3C{-}N{=}OH^+\ \mathbf{8}) = 903 \pm 12$ kJ mol^{-1} and $\Delta_f H^\circ_0(H_2\underbracket{C{-}NH{-}O}H^+\ \mathbf{2\Delta}) = 918 \pm 12$ kJ mol^{-1}.

Isomerizations and fragmentations of $[CH_4NO]^+$ ions

The entities **2**, **3**, **8** and **9** could be interconverted to each other by 1,2- or 1,3-hydrogen migration (Scheme 1). The 1,3-H-shift connecting **2** with **9** requires the largest critical energy (> 260 kJ mol^{-1}). A TS for the 1,3-H-shift linking **3** with **8** could not be located. The energy barriers for 1,2-H-shifts are consistently smaller (Fig. 3).

Starting from **8**, the least stable of the three protonated formaldehyde oximes, two isomerization channels are opened: the path **8**→**2** involving a shift from C to N is much preferred over the path **8**→**9** which involves an O to N shift. Migration of a proton onto a more electronegative centre is clearly favoured over the reverse situation. Particularly relevant to the BR is the interconversion between **2** and **3**. The least energy demanding route passes through a 1,2-H-shift and needs to overcome an energy barrier of *ca.* 148 kJ mol^{-1} relative to **3**; the TS **2/3** lies only 14 kJ mol^{-1} higher in energy than the TS **2/8**. Within the error bars of our calculations, both isomerizations **2**→**3** and **2**→**8** can be seen as competitive.

The ring-closure of **2** giving the three-membered ring **2Δ** is associated with a substantial barrier height (168 kJ mol^{-1}). In the opposite direction, the ring-opening of **2Δ** has to overcome a more moderate barrier of 88 kJ mol^{-1}. For its part, the ion **9** is extremely stable lying in profound potential wells; its direct conversion to the more stable isomer **2** is less favoured by 28 kJ mol^{-1} than the two-step path **9**→**8**→**2**.

Overall the present calculations suggest that the $[CH_4NO]^+$ ion isomers considered are separated from each other by rather significant energy barriers for hydrogen migrations and that a direct 1,2-H shift constitutes the easiest pathway linking both *N*- and *O*-protonated formaldehyde oximes **2** and **3** with barrier height of 148 kJ mol^{-1} relative to **3** (or 225 kJ mol^{-1} relative to **2**). The alternative routes involving other isomers could be ruled out. With regard to the fragmentations, the conversion of the oxonium ion **3** to the complex product **5** is possible *via* two distinct reaction mechanisms: while the first is the BR as discussed in ref. 4, the second channel is a concerted 1,2-*cis* elimination. In some ways, the BR could be regarded as a *trans*-elimination. The elimination TS **3/5**-Elim exhibits a significantly elongated N–O distance (2.218 Å), but a shorter C–H distance (1.142 Å), indicative of an asynchronous process. Examination of the intrinsic reaction coordinate (IRC) pathway indicates that when the transition point is passed, a proton is actually transferred from C to O forming some intermediate structures whose geometry resembles $(HCN\cdots HOH_2^+)$ **5**. The energetics presented in Fig. 4 clearly show that the BR of **3** remains favoured over the *cis*-elimination. The energy difference of 34 kJ mol^{-1} between both TS **3/5**-BR and **3/5**-Elim points toward an unambiguous predominance of the BR in the transformation of the oxonium ion **3**. The H_2-loss process from **3** could be ruled out due to its very high barrier. A direct transformation **2**→**5** is also possible through a concerted 1,2-elimination; the corresponding TS **2/5** exhibits some marked differences with the TS **3/5**-Elim. In **2/5**, the C–H bond is practically broken whereas the N–O distance remains almost intact, in clear contrast with the situation in **3/5**-Elim discussed above. The **2**→**5** conversion is associated with a high barrier of 288 kJ mol^{-1} relative to **2**; the latter value is *ca.* 63 kJ mol^{-1} larger than that for the 1,2-H-shift connecting **2** with **3**. Accordingly, the elimination from **2** is also an unlikely route leading to the product **5**. Note that in a concerted *cis*-elimination, a process often occurring in the gas phase chemistry of oxonium and ammonium cations;[11] the departure of both moieties form primarily an ionic entity (such as H_3O^+), which is possibly easier to achieve than that forming a neutral group (such as H_2O). Proceeding from **2**, the most favoured dissociation turns out to be the **2**→**3**→**5** route in which the initial 1,2-H-shift is rate-determining (Fig. 4). In the event that the metastable oxonium ions **3** could be generated by another means, it could readily undergo a BR. Owing to the formation of a stable ion complex **5** as the product, this process should be characterized by a small kinetic energy release (KER).

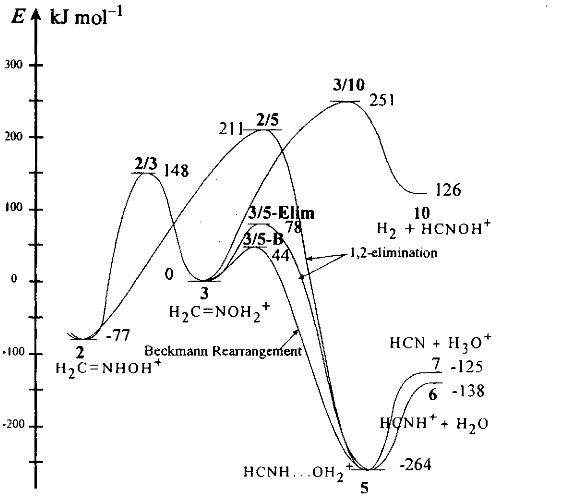

Fig. 4 Schematic potential energy profiles for fragmentations of both *N*- and *O*-protonated formaldehyde oximes. Values at the MP4/6-311++G(d,p) + ZPE level.

It can thus be concluded that the gas-phase Beckmann rearrangement, initiated by protonation of formaldehyde oxime, is a two-step transformation in which the conversion of the *N*-protonated form **2** to the *O*-protonated form **3** is the most energy demanding step. The estimated energy barrier of 225 kJ mol^{-1} is not consistent with the experimental activation energy of *ca.* 100 kJ mol^{-1} measured for the BR of substituted oximes in different media.[3] This indicates the crucial role of either the substituents or the solvent in accelerating the BR. The conversion of the *O*-protonated oxime to the products, commonly assumed up to now to be the BR, is the most facile of all the processes considered.

With regard to the *N*-protonated nitrosomethane **9**, we would

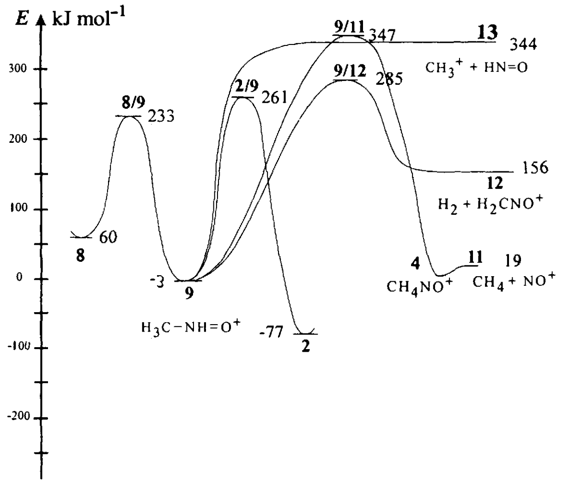

Fig. 5 Schematic potential energy profiles for rearrangements of the *N*-protonated nitrosomethane. Values at the MP4/6-311 + + G(d,p) + ZPE level.

like to take this opportunity to have another look at its rearrangement pathways. Reaction (5), which is the simplest

$$CH_4 + NO^+ \ \mathbf{11} \longrightarrow CH_3\text{-}NH{=}O^+ \ \mathbf{9} \longrightarrow CH_3N{=}O + H^+ \quad (5)$$

model for the electrophilic substitution of aliphatic hydrocarbons, has recently been investigated in detail by the use of *ab initio* calculations.[6]

It has been reported that two distinct reaction paths converting **11** to **9** are possible: while the first is an insertion of NO$^+$ into C–H bond, the second path with a lower energy barrier than the first involves a very shallow minimum energy structure which structurally resembles either a complex between H$_2$CNO$^+$ and H$_2^+$ or a complex between CH$_4$ and NO$^+$ resulting from an attack of N to C. However this intermediate is much higher in energy than these fragments.[6] The second pathway is, as a consequence, a multi-step transformation [reaction (6)]. Although the existence of such an (unstable)

$$CH_4 + NO^+ \ \mathbf{11} \longrightarrow CH_3\text{-}N{=}OH^+ \ \mathbf{8} \longrightarrow CH_3NH{=}O^+ \ \mathbf{9} \quad (6)$$

intermediate is not quite certain, it has been concluded[6] that the electrophile NO$^+$ cation attacks methane at carbon rather than at a C–H bond.

As seen in the energy profiles illustrated in Fig. 5, while the direct insertion of NO$^+$ into a C–H bond converting **11** to *N*-protonated nitromethane **9** could be confirmed, we have not been able to confirm the existence of the intermediate reported in ref. 6 as an energy minimum at the levels of theory employed in this work. On the other hand, we also could not locate a TS connecting CH$_4$ + NO$^+$ with the *O*-protonated nitrosomethane **8**. In other words, we do not have a convincing result to support the proposition that the CH$_4$ + NO$^+$ reaction would prefer an initial C-attack over a C–H insertion. In any case, the latter process has, in the gas phase, an extremely large energy barrier (328 kJ mol^{-1}, Fig. 5), and this indicates that the solvent should play a crucial role in the reactions in solution.

Conclusions

The present detailed exploration of the [CH$_4$NO]$^+$ potential energy surface confirms that the classical Beckmann rearrangement represents in the gas phase the easiest way of transforming protonated oximes and their isomers into products. This reaction mode should be taken into consideration in the rationalization of the unimolecular chemistry of the analogous classes of cations.

Acknowledgements

The authors are grateful to the Belgian Science Foundations (NFWO and IWT) and the Belgian Government (DWTC) for continuing support.

References

1 E. Beckmann, *Chem. Ber.*, 1886, **19**, 988.

2 For recent comprehensive reviews, see *e.g.* (*a*) R. E. Gawley, *Org. React.*, 1987, **35**, 1; (*b*) M. Hesse, in *Ring Englargement in Organic Chemistry*, VCH, Weinheim, 1991.

3 (*a*) W. Z. Heldt, *J. Org. Chem.*, 1961, **26**, 1695; (*b*) M. I. Vinnik and N. G. Zaralchni, *Russ. Chem. Rev.* (*Engl. Transl.*), 1967, **36**, 51.

4 M. T. Nguyen and L. G. Vanquickenborne, *J. Chem. Soc.*, *Perkin Trans. 2*, 1993, 1969.

5 M. T. Nguyen, *Int. J. Mass Spectrom. Ion Processes*, 1994, **136**, 45.

6 P. R. Schreiner, P. v. R. Schleyer and H. F. Schaefer, *J. Am. Chem. Soc.*, 1993, **115**, 9659.

7 M. J. Frisch, M. Head-Gordon, G. W. Trucks, J. B. Foresman, H. B. Schlegel, K. Raghavachari, M. Robb, J. S. Binkley, C. Gonzalez, D. J. DeFrees, D. J. Fox, R. A. Whiteside, R. Seeger, C. F. Melius, J. Baker, R. L. Martin, L. R. Kahn, J. J. B. Stewart, S. Topiol and J. A. Pople, GAUSSIAN 90, Gaussian Inc., Pittsburgh, PA, 1990.

8 S. G. Lias, J. E. Bartmess, J. F. Liebmann, J. L. Holmes, R. D. Levin and W. G. Wallard, *J. Phys. Chem. Ref. Data*, 1988, 17, Supplement 1.

9 A. H. Otto, *J. Mol. Struct.*, *Theochem.*, 1991, **235**, 489.

10 (*a*) M. T. Nguyen, J. Rademakers and J. M. L. Martin, *Chem. Phys. Lett.*, 1994, **221**, 149; (*b*) B. J. Smith, J. A. Pople, L. A. Curtius and L. Radom, *Aust. J. Chem.*, 1992, **45**, 285; (*c*) R. A. Peerboom, S. Ingemann, N. M. N. Nibbering and J. F. Liebman, *J. Chem. Soc.*, *Perkin Trans. 2*, 1990, 1825.

11 M. T. Nguyen, L. G. Vanquickenborne and G. Bouchoux, *Int. J. Mass. Spectrom. Ion Processes*, 1993, 124, R11.

Paper 5/01679G
Received 16*th March* 1995
Accepted 5*th May* 1995